Chapter 4

Methods

4.1 Introduction

This chapter consists of three discrete sections. The first section details the development of a computer model to predict forces applied to the pedals of an isokinetic cycle ergometer by paraplegic individuals in response to stimulation of the quadriceps, hamstring and gluteal muscles. While much of the discussion specifying why particular equations were chosen has already been outlined in the literature review, this chapter explains how these equations were compiled into a unified musculo-skeletal model.

The second part of this chapter describes the methodology used in experiments involving isokinetic knee extension tests of paraplegic individuals using stimulation of just the quadriceps muscles. These experiments were designed to generate data under controlled conditions that could be used to validate certain equations within the musculoskeletal model. This data set will also be used in Chapter 6 to derive and/or verify constants within the equations for modelling the muscles of paraplegic individuals activated via NMES. The process for fitting constants is not described in Chapter 4 because the methods used for each equation were often dependent upon analysis of prior results. Therefore, only the method for generating the data sets will be described in the present chapter.

The final portion of Chapter 4 outlines experiments performed on an isokinetic cycle ergometer. Data from these experiments will be used in Chapter 7 to validate the complete cycling model.

4.2 Computer Simulations

A forward dynamic model was developed to simulate the dynamics of paraplegic individuals cycling an isokinetic cycle ergometer using NMES to activate the quadriceps, hamstrings and gluteal muscles. The lower limbs were modelled as two rigid segments connecting the hip joint to a bicycle crank. Quadriceps, hamstring and gluteal muscles were modelled using a single effective muscle per group and integrated with the segmental dynamics to predict pedal forces resulting from specific muscle stimulation sequences. All simulation equations were derived and executed using Mathematica 3.0 (Wolfram Research, Inc).

The ergometer used for this experiment allowed the following three assumptions to be used to simplify the model:

Simplifying Assumptions

1. The hip joint was fixed in space.
   A fixed hip position has been a common assumption in previous upright cycling models (eg. Kautz and Hull, 1993; Raasch et al., 1997). The broad seat and back support on the present recumbent ergometer fixed the hip in space better than a conventional bicycle seat, supporting the use of a fixed hip position for the present model.

2. The leg consisted of two segments connecting the hip to the ergometer crank.
   The ergometer utilised a brace around the ankle and foot to hold the legs in place during cycling. As well as restricting movement away from the sagittal plane, this brace effectively fixed the ankle joint meaning that the shank and foot could be modelled as a single segment.

3. The ergometer crank rotated at a constant angular velocity.
   The motor on the ergometer was supposed to hold the velocity of the crank constant, whether a subject was actively pedalling or not. While the ergometer did not maintain velocity completely constant, Section 7.2.2 discusses this in some detail and concludes that the effects of crank velocity changes on model performance were relatively minor.

These three assumptions meant that the angles of the thigh and shank were uniquely determined by crank angle. Regardless of the level of muscle force, the crank of an isokinetic ergometer would continue to rotate at a constant velocity. Thus, the leg displacements would be unaffected by muscle activation. This assumption allowed segment kinematics to be defined in advance of muscle forces with no feedback from forces back to kinematics. The assumptions of hip location and crank velocity are discussed extensively in Section 7.2.2. Section 7.6 demonstrates that the assumption of fixed segment lengths had little effect on predictions made by the model.

The overall simulation involved three sub-models: a kinematic model, a muscle model, and a kinetic model. The kinematic model determined segment displacements and hence overall muscle-tendon lengths. The muscle model determined the force of contraction from imposed stimulation patterns and muscle lengths generated by the kinematic model. The kinetic model then determined external pedal forces from the muscle forces and segment displacements. As mentioned earlier, there was no feedback from the kinetic model to the kinematic model.

4.2.1 Kinematic Model

Segment Displacements

The lower limbs were modelled as two rigid segments connecting a fixed hip joint to a bicycle crank. The model was considered planar with simple hinge joints at the knee and between the foot and crank (Figure 4.2.1.1).

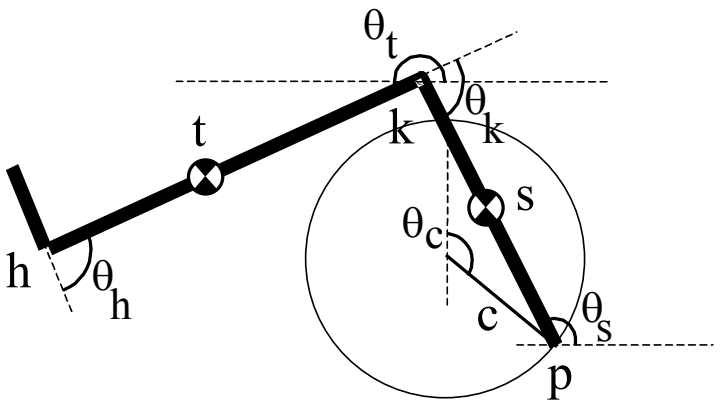

Figure 4.2.1.1 Illustration of segments included in the kinematic model.

The kinematic model was derived from three pairs of second order differential equations. These equations describe the horizontal and vertical accelerations of the centres of mass of the thigh and shank, as well as the acceleration of the crank axle (equal to zero), as a function of segment angular velocities and accelerations, measured from the stationary hip.

$$\ddot{x}_t = \dot{\theta}_t^2 r_t \mathrm{Cos}[\theta_t] + \ddot{\theta}_t r_t \mathrm{Sin}[\theta_t]$$

Equation 4.2.1.1

$$\ddot{y}_t = \dot{\theta}_t^2 r_t \mathrm{Sin}[\theta_t] - \ddot{\theta}_t r_t \mathrm{Cos}[\theta_t]$$

Equation 4.2.1.2

$$\ddot{x}_s = \dot{\theta}_t^2 l_t \mathrm{Cos}[\theta_t] + \ddot{\theta}_t l_t \mathrm{Sin}[\theta_t] + \dot{\theta}_s^2 r_s \mathrm{Cos}[\theta_s] + \ddot{\theta}_s r_s \mathrm{Sin}[\theta_s]$$

Equation 4.2.1.3

$$\ddot{y}_s = \dot{\theta}_t^2 l_t \mathrm{Sin}[\theta_t] - \ddot{\theta}_t l_t \mathrm{Cos}[\theta_t] + \dot{\theta}_s^2 r_s \mathrm{Sin}[\theta_s] - \ddot{\theta}_s r_s \mathrm{Cos}[\theta_s]$$

Equation 4.2.1.4

$$0 = \dot{\theta}_t^2 l_t \mathrm{Cos}[\theta_t] + \ddot{\theta}_t l_t \mathrm{Sin}[\theta_t] + \dot{\theta}_s^2 l_s \mathrm{Cos}[\theta_s] + \ddot{\theta}_s l_s \mathrm{Sin}[\theta_s] + \dot{\theta}_c^2 l_c \mathrm{Cos}[\theta_c] + \ddot{\theta}_c^2 l_c \mathrm{Sin}[\theta_c]$$

Equation 4.2.1.5

$$0 = \dot{\theta}_t^2 l_t \mathrm{Sin}[\theta_t] - \ddot{\theta}_t l_t \mathrm{Cos}[\theta_t] + \dot{\theta}_s^2 l_s \mathrm{Sin}[\theta_s] - \ddot{\theta}_s l_s \mathrm{Cos}[\theta_s] - \dot{\theta}_c^2 l_c \mathrm{Sin}[\theta_c] + \ddot{\theta}_c^2 l_c \mathrm{Cos}[\theta_c]$$

Equation 4.2.1.6

Equations 4.2.1.1 to 4.2.1.6 were solved simultaneously to give angular acceleration of the shank and thigh as a function of crank angle as Equations 4.2.1.7 and 4.2.1.8. Crank angular acceleration has been included in Equation 4.2.1.5 and Equation 4.2.1.6, however Equations 4.2.1.7 and 4.2.1.8 were simplified by assuming that crank acceleration was equal to zero for an isokinetic ergometer.

$$\ddot{\theta}_s = \frac{\dot{\theta}_c\, l_c\, Csc[\theta_s - \theta_t]\, \left(Cot[\theta_s - \theta_t]\, Sin[\theta_c + \theta_t]\left(\dot{\theta}_s - \dot{\theta}_t\right) - Cos[\theta_c + \theta_t]\left(\dot{\theta}_c + \dot{\theta}_t\right)\right)}{l_s}$$

Equation 4.2.1.7

$$\ddot{\theta}_t = \frac{\dot{\theta}_c\, l_c\, Csc[\theta_s - \theta_t]\, \left(Cos[\theta_c + \theta_s]\left(\dot{\theta}_c + \dot{\theta}_s\right) - Cot[\theta_s - \theta_t]\, Sin[\theta_c + \theta_s]\left(\dot{\theta}_s - \dot{\theta}_t\right)\right)}{l_t}$$

Equation 4.2.1.8

The kinematic model was solved by giving initial values for shank and thigh angle, and then iteratively finding angular displacements and velocities of the segments, as a function of time, that satisfied Equations 4.2.1.7 and 4.2.1.8. This was achieved using the NDSolve function of Mathematica. Initial angles of the thigh and shank for this numerical solution were determined by simultaneously solving Equations 4.2.1.9 to 4.2.1.12

$$\left(x_k^2 - x_p^2\right)^2 + \left(y_k^2 - y_p^2\right)^2 = l_s^2$$

Equation 4.2.1.9

$$\left(x_k^2 - x_h^2\right)^2 + \left(y_k^2 - y_h^2\right)^2 = l_t^2$$

Equation 4.2.1.10

$$\theta_s = \text{ArcTan}\left[\frac{\left(y_k - y_p\right)}{\left(x_k - x_p\right)}\right] + \Pi$$

Equation 4.2.1.11

$$\theta_t = \text{ArcTan}\left[\frac{\left(y_h - y_k\right)}{\left(x_h - x_k\right)}\right] + \Pi$$

Equation 4.2.1.12

There were two possible solutions to these equations, hence the solution that avoided hyperextension of the knee was always chosen.

In summary, the kinematic model predicted the angular displacement, velocity and acceleration of the thigh, shank and crank as functions of time. In order to run the model, the length of the shank, thigh and crank; the relative positions of the hip and crank axle; the angular velocity of the crank and initial crank angle had to be specified. The kinematic model was able to run independent of the muscle model because of the isokinetic ergometer and the fixed ankle position.

Muscle Lengths

Once the segment kinematics have been determined, kinematics of a whole muscle-tendon unit can be calculated provided the moment arm of a muscle is known as a function of joint angle. Available literature was used to develop muscle moment arm equations for each muscle at each joint crossed by that muscle (Section 2.4.1). Moment arm equations were calculated from joint angular displacements and expressed as functions of time. Muscle tendon kinematics were then calculated by numerical solution of a differential equation giving the rate of muscle tendon length change as a function of the angular velocities of the joints spanned by that muscle. For example, hamstring length was calculated by forward solution of Equation 4.2.1.13. Initial muscle-tendon lengths for the differential equations were calculated from Hawkins and Hull, 1990.

$$lmth'[t] = qk'[t] \times dhk[t] - qh'[t] \times dhh[t]$$

Equation 4.2.1.13

4.2.2 Muscle Model

The muscle model is represented in Figure 4.2.2.1. Feedback from the tendon force to the length of the muscle and tendon is shown as a dotted line because that feedback was not used in the present model; muscle-tendon kinematics were determined in advance by the segment kinematics model. Figure 4.2.2.1 shows that muscle-tendon kinematics and muscle activation provide two inputs to the model and these determine the force of contraction. There is a feedback loop from tendon length to fibre length, hence the model must solve this iteratively to generate a continuous solution.

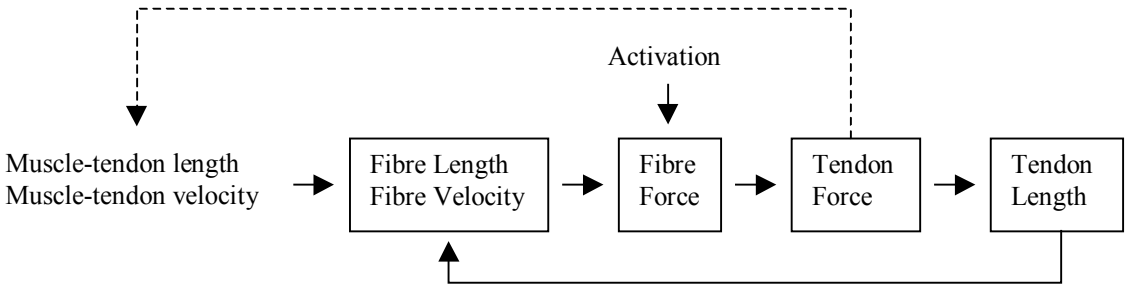

Figure 4.2.2.1 The conceptual muscle model.

Figure 4.2.2.2 illustrates how the muscle model was coded. As per Figure 4.2.2.1, the only free inputs to the model are muscle-tendon kinematics and muscle activation. All other variables are controlled by these two.

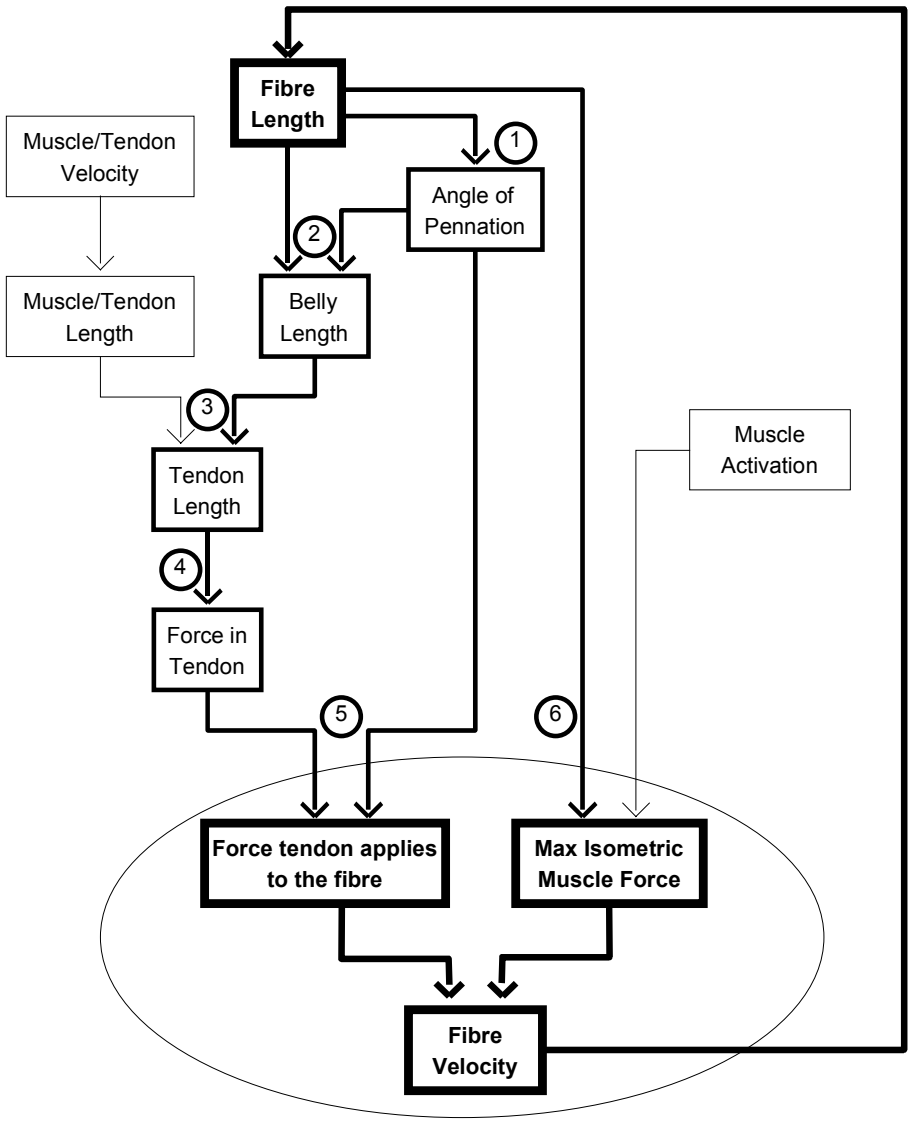

Figure 4.2.2.2 Schematic of muscle model code. The numbers in this figure refer to the Accessory Equations described below

The model was centred around a first order differential equation giving fibre velocity as a function of tendon force and the maximum isometric force a muscle is capable of at a given length (Hill's equation; Stern, 1974). This is the component of the model within the dashed ellipse in Figure 4.2.2.2. The differential equation was solved iteratively over time to give fibre length as a function of time. As time progressed, each new value for fibre length, together with the model inputs (muscle activation and muscle-tendon kinematics), was used to calculate a resulting fibre velocity which led to the next fibre length. Thus, the model consisted of the force velocity equation, together with a number of accessory equations to

predict tendon force and fibre isometric force from a given fibre length. Whole muscle kinematics and activation patterns provided inputs to the model. Mathematica code for the muscle model may be viewed in Appendix 2.

Fibre velocity equation

The fibre velocity equation took one of three forms depending on the difference between fibre contraction force (tending to shorten the muscle) and tendon force (lengthening the muscle). The three forms are given by Equations 4.2.2.1 and 4.2.2.1

1. If fibre force > tendon force then concentric contraction,

$$lf'[t] = \frac{b(ftom[t] - ffol[t])}{a\, a[t] + ftom[t]}$$

(Stern, 1974)

Equation 4.2.2.1

2. If fibre force < tendon force then eccentric contraction,

$$lf'[t] = \frac{b\,(1 - ecc)\, ffol[t]\,(-ffol[t] + ftom[t])}{(a + ffol[t])\,(-(ecc \times ffol[t]) + ftom[t])}$$

(Pierrynowski and Morrison, 1985)

Equation 4.2.2.2

3. If tendon force/fibre force > 1.25 then correct overshoot

$$lf'[t] = 1$$

Equation 4.2.2.3

Fibre velocity may become infinitely large as tendon force increases. The form of Pierrynowski and Morrison's equation sets this infinite velocity to be reached when tendon force/fibre force equals 1.25 (the ratio of maximum eccentric force to isometric force). While solving the differential equation, Mathematica sometimes uses fibre length step sizes that may

cause the eccentric/isometric force ratio to become greater than 1.25. This causes a negative fibre velocity instead of the required positive value and the model subsequently freezes. If the effective step size was set infinitely small then this would not occur, however the model would take infinitely long to evaluate. The third form of the force - velocity equation was therefore an error trap to prevent the step size overshooting the allowable range of force. This forced Mathematica to use smaller step sizes where appropriate to prevent discontinuity, thus remaining to the left of the asymptote on Figure 4.2.2.3. It should be emphasised that the third form never eventuated in a final solution. In order to maintain a continuous function, Mathematica chose smaller step sizes that resulted in the second form being used throughout all eccentric contractions. The third form was useful only to force the code to use appropriate step sizes when tracking the second form of the force - velocity equation.

The initial fibre length was set at optimum fibre length for each simulation. From this starting position, the model changed rapidly to a more appropriate fibre length, usually within 0.1 s. The first period of every simulation was always discarded in order to miss this transition period.

Figure 4.2.2.3 illustrates the predicted fibre velocity as a function of tendon force. Note that, for tendon forces less than the isometric strength of the muscle at a particular length and level of activation, the muscle will shorten (negative velocity). The muscle will lengthen at ever increasing velocities when tendon force is greater than isometric strength. The maximum force able to be exerted during an eccentric contraction has been limited to 125% isometric strength (Pierrynowski and Morrison, 1985).

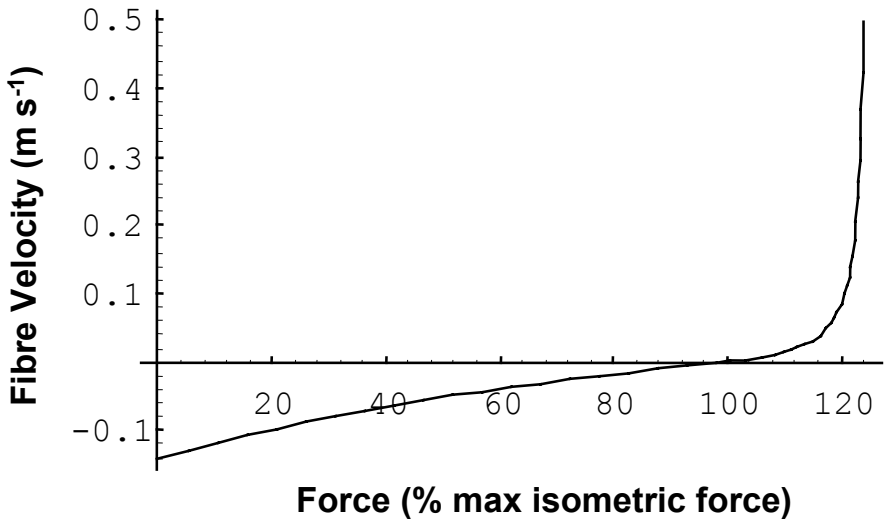

Figure 4.2.2.3 Muscle fibre velocity expressed as a function of the force applied to a fibre.

Activation

Activation provided an independent input to the muscle model with timing controlled as a function of crank angle (Figure 4.2.2.2). Because crank kinematics were determined in advance of the muscle model, activation was also known in advance (hence it was independent to the muscle model). Muscle stimulation was modelled as on/off, however a muscle does not become fully activated as soon as it is switched on. The rise in muscle activation was modelled using a first order differential equation adapted from Pandy et al. (1990). Pandy et al.'s method was modified to include a delay between stimulation onset/offset and the rise/fall of muscle force (Equation 4.2.2.4).

$$\frac{d\,a[t]}{d\,t} = \text{If } \; a\left[t - \text{delay}\right] = 1,$$

$$\text{Then } \frac{1-a}{\tau_{rise}},$$

$$\text{Else } \frac{a_{min} - a}{\tau_{fall}}$$

Equation 4.2.2.4

In order to allow a different delay constant for stimulation onset and cessation, Equation 4.2.2.4 had a further nested “If” statement to select the appropriate delay constant. Full details of this equation and the constants used may be found in Section 6.1.8. Figure 4.2.2.4 illustrates the response of muscle activation to stimulation switching on and off as described by Equation 4.2.2.4.

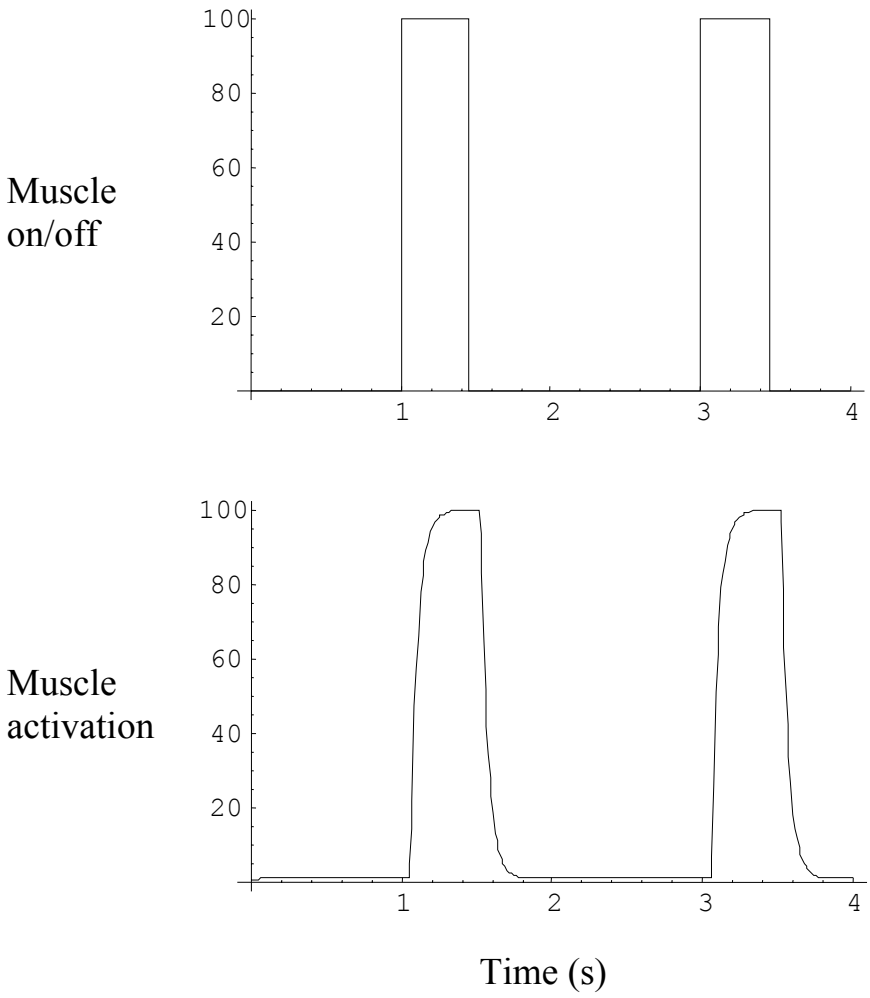

Figure 4.2.2.4 Illustration of muscle activation in response to stimulation.

Accessory Equations

A number of equations were required to calculate the force with which a muscle may contract given a particular fibre length, muscle-tendon length and level of activation. The use of these equations is illustrated in Figure 4.2.2.2 and each is numbered according to this figure.

① *Angle of Pennation as a function of fibre length.*

$$\text{pennang}[t] = \text{ArcCsc}\left[\frac{\text{lf}[t]\ \text{Csc}[\text{pennango}]}{\text{lfo}}\right]$$

Equation 4.2.2.5

Equation 4.2.2.5 comes from rearranging Equation 4.2.2.6, derived from Pierrynowski and Morrison (1985). Equation 4.2.2.6 assumes that angle of pennation changes with fibre length but muscle thickness remains constant as illustrated by Figure 4.2.2.5 (See Section 2.4.3).

Figure 4.2.2.5 Schematic of muscle belly length. As the belly shortens, the thickness remains constant and hence pennation angle increases.

$$\mathrm{Sin}[\alpha_o] = \frac{T}{lf_o}$$

$$\therefore T = lf_o \mathrm{Sin}[\alpha_o]$$

$$\mathrm{Sin}[\alpha] = \frac{T}{lf}$$

$$\therefore lf = \frac{T}{\mathrm{Sin}[\alpha]}$$

$$= \frac{lf_o \mathrm{Sin}[\alpha_o]}{\mathrm{Sin}[\alpha]}$$

Equation 4.2.2.6

② *Muscle belly length as a function of fibre length and angle of pennation*

$$lb[t] = lf[t]\ Cos[pennang[t]]$$

Equation 4.2.2.7

This definition gives an effective belly length for a single fibre. Its role is simply to define the length of tendon in series with the fibre. See Section 2.4.2 for discussion of alternative models and their respective implications.

③ *Tendon Length as a function of Muscle-tendon length and belly length.*

$$lt[t] = \begin{array}{ll} \text{If} & lmt[t] - lb[t] > slt \\ \text{then} & lmt[t] - lb[t] \\ \text{else} & slt \end{array}$$

Equation 4.2.2.8

The "If" statement in Equation 4.2.2.8 prevents the tendon from shortening below resting length when the muscle is at short lengths.

④ *Tendon force as a function of tendon length*

$$ft[t] = kt\ (lt[t] - slt)$$

Equation 4.2.2.9

This linear equation implies constant tendon stiffness. While this assumption is unlikely to be correct given the low force levels involved, there is limited data available to quantify an alternative, non-linear equation. This is particularly so for the de-enervated muscles currently being modelled (Section 2.4.2).

⑤ *Force a tendon applies to its fibre.*

$$ftom[t] = \frac{ft[t]}{Cos[pennang[t]]}$$

Equation 4.2.2.10

Because the fibre is not necessarily orientated parallel to the tendon, a fibre must apply more force to a tendon than is transmitted along the tendon. Equation 4.2.2.10 quantifies the amount of force the fibre generates in order to generate a given tendon force. This term has been adapted from Pierrynowski and Morrison (1985).

⑥ *Maximum isometric muscle force as a function of fibre length*

$$ffol[t] = ffo\ a[t]\ fleqtn[lf[t]/lfo]$$

Equation 4.2.2.11

Isometric force at a given length is modelled as the product of muscle strength, level of activation and relative force for a given fibre length. Strength of individual muscles were adjusted for each simulation to match measured outcomes. Activation level came from Equation 4.2.2.4 and the force-length relationship derived from Delp et al. (1990).

The accessory equations were defined in advance of solving the fibre velocity equation so that they could be called where necessary when solving the fibre velocity equation. An example of how the muscle model was coded may be viewed in Appendix 2.

4.2.3 Kinetic Model

The kinetic model took inputs from the kinematic and muscle models to predict forces applied to the right pedal. This model was based on Newton's equations of motion applied to the thigh and shank segments, giving six equations defining motion of the two segments.

$$F_{hx} - F_{kx} = m_t \ddot{x}_t$$

Equation 4.2.3.1

$$F_{hy} - F_{ky} = m_t \ddot{y}_t + m_t g$$

Equation 4.2.3.2

$$F_{hy} r_t \text{Cos}[\theta_t] - F_{hx} r_t \text{Sin}[\theta_t] + F_{ky} (l_t - r_t) \text{Cos}[\theta_t] - F_{kx} (l_t - r_t) \text{Sin}[\theta_t] = I_t \ddot{\theta}_t + M_h + M_k$$

Equation 4.2.3.3

$$F_{kx} - F_{px} = m_s \ddot{x}_s$$

Equation 4.2.3.4

$$F_{ky} - F_{py} = m_s \ddot{y}_s + m_s g$$

Equation 4.2.3.5

$$F_{ky} r_s \text{Cos}[\theta_s] - F_{kx} r_s \text{Sin}[\theta_s] + F_{py} (l_s - r_s) \text{Cos}[\theta_s] - F_{px} (l_s - r_s) \text{Sin}[\theta_s] = I_s \ddot{\theta}_s - M_k$$

Equation 4.2.3.6

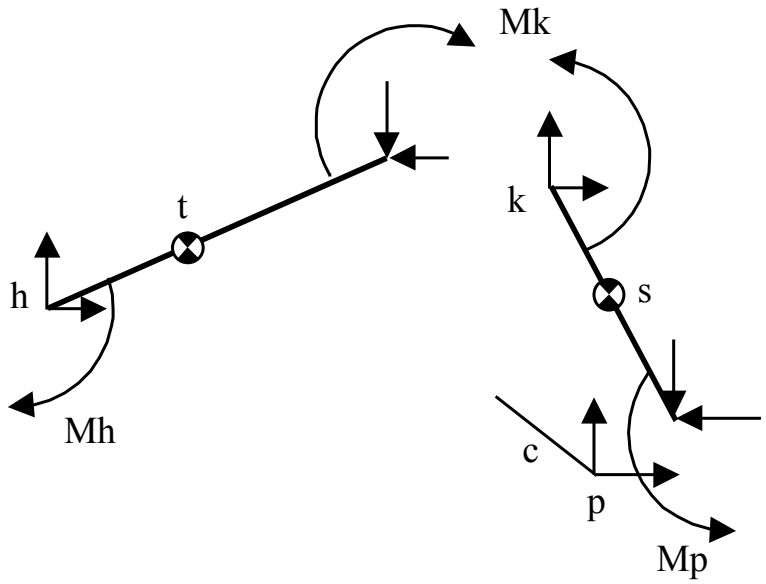

Figure 4.2.3.1 Illustration of the positive direction for all variables used in Equations 4.2.3.1 to 4.2.3.6. Note: Torques and forces across the knee act on both the shank and thigh segments. The direction of positive knee forces and torques are shown as they act on both segments. Similarly, pedal forces act on both the shank and crank, so are illustrated as positive forces on both segments[1].

Equations 4.2.3.1 to 4.2.3.6 were solved simultaneously to give vertical and horizontal pedal forces as a function of kinematic variables (Equations 4.2.3.7 and 4.2.3.8).

fpx[t] =

(Cosec[qs[t]]× (-(is×aas[t]) + ms×rs×(g + asy[t])×Cos[qs[t]] mk[t] - ms×rs×asx[t]×Sin[qs[t]]))/ls +

(Cotan[qs[t]]× Cosec [qs[t] - qt[t]]×(lt×(-(is×aas[t]) + ms×rs×(g + asy[t])×Cos[qs[t]] + mk[t] - ms×rs×asx[t]×Sin[qs[t]])×Sin[qt[t]] - ls×Sin[qs[t]]× (-(it×aat[t]) + lt×ms×(g + asy[t])×Cos[qt[t]] + mt×rt×(g + aty[t])×Cos[qt[t]] - mh[t] - mk[t] - lt×ms×asx[t]×Sin[qt[t]] - mt×rt×atx[t]×Sin[qt[t]]))/(ls×lt)

Equation 4.2.3.7

[1] Vertical pedal force (fpy) is given as positive upwards within this section, as illustrated by Figure 4.2.3.1, and in the model software included in Appendix 2.1. Measured pedal forces reported in Chapter 7 were calculated using a positive downwards convention. All modelled pedal forces were converted to the downwards convention before comparison in later chapters.

fpy[t] =

(Cosec [qs[t] - qt[t]]× (lt×(-(is×aas[t]) + ms×rs×(g + asy[t])×Cos[qs[t]] + mk[t] - ms×rs×asx[t]×Sin[qs[t]])×Sin[qt[t]] - ls×Sin[qs[t]]× (-(it×aat[t]) + lt×ms×(g + asy[t])×Cos[qt[t]] + mt×rt×(g + aty[t])×Cos[qt[t]] - mh[t] - mk[t] - lt×ms×asx[t]×Sin[qt[t]] - mt×rt×atx[t]×Sin[qt[t]]))/(ls×lt)

Equation 4.2.3.8

In order to eliminate the effects of inertial factors and produce nett pedal forces resulting from muscle actions, the mass of each segment was set to zero. This procedure was valid only with the assumption that the isokinetic ergometer kept inertial effects constant irrespective of muscle force generation. Nett forces were used in order to avoid the difficulty in estimating segment inertial parameters for paraplegic individuals (Tashman, 1992).

Propulsive torque applied to the crank was calculated from pedal forces and crank angles using Equation 4.2.3.9.

$$\text{torq}[t] = \left(\text{fpx}[t] \times \text{Cos}[\text{qc}[t]] - \text{fpy}[t] \times \text{Cos}[\text{qc}[t]]\right) \times \text{lc}$$

Equation 4.2.3.9

4.2.4 Summary

The present computer simulations enabled prediction of pedal forces, and hence torque and power, applied to the crank of an isokinetic cycle ergometer. Simulations required initial inputs of anthropometric parameters specifying the length of segments and the relative position of the hip and the crank axle. This information, together with angular velocity of the crank, enabled all kinematic variables to be calculated as functions of time. The assumptions of isokinetic cycling and fixed hip position allowed these kinematic calculations to be performed without any feedback from subsequent kinetic calculations. The kinematic model provided estimates of muscle lengths as functions of time. This information, together with stimulation firing angles, was used to calculate muscle tendon forces as functions of time. Finally, tendon forces were combined with segmental dynamics within the kinetic model to calculate the forces and consequent torque applied to the ergometer's pedals.

4.3 Knee Extension Experiments

4.3.1 Equipment

Experiments were conducted using a Biodex Isokinetic Dynamometer (Biodex Medical Systems). Contractions were elicited in the quadriceps muscles using the Exstim percutaneous muscle stimulator (T Turner, The University of Sydney). Constant voltage, monophasic, square wave stimulation pulses of 250 μs were delivered at a frequency of 35 Hz using moistened 8 × 13 cm self adhesive electrodes (Empi, Cat No 86906350) placed over the belly of the quadriceps muscles (Figure 4.3.1.1). Current amplitude was adjusted as outlined in section 4.3.4.

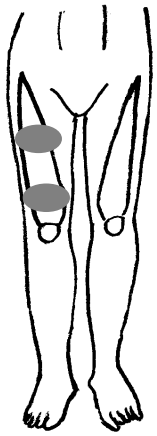

Figure 4.3.1.1 Illustration of electrode placements.

Output from the stimulator was monitored via an optically isolated DC voltage proportional to the current and voltage levels delivered to the subject. This monitoring signal was derived from a sample and hold circuit that reset in response to a TTL pulse from the stimulator. The monitoring signal thus allowed determination of stimulation onset and cessation, together with an accurate measure of the current and voltage delivered. The dynamometer was fitted with an analogue output that enabled sampling of a DC voltage proportional to torque and dynamometer angle. DC voltage signals from the output from the dynamometer and the

muscle stimulator were sampled simultaneously using an IBM compatible personal computer (Intel, 80386), 12 bit analogue to digital converter (DT2801, Data Translation) and ADS software (Motion Analysis Corp).

4.3.2 Subjects

Seven SCI subjects (1 female, 6 males) with lesions between vertebrae T4 and T9 were recruited for this study (6 classified ASIA - A, 1 ASIA - B. Ditunno et al., 1994). All participants underwent informed consent procedures according to the guidelines of the University of Sydney Human Ethics Committee and received medical screening for pre-existing musculo-skeletal or cardiorespiratory disorders before participating in the study. All subjects had previously trained regularly using NMES, however not all were in regular training at the time of the experiment.

4.3.3 Calibration

Angle and torque outputs from the dynamometer were calibrated at each session by placing the dynamometer arm in known positions and hanging static weights from the arm. The voltage outputs from the dynamometer were linear for both torque and angle with an R^2 better than 0.999. An example calibration set is given in Appendix 3.1. Anatomical knee angles were set at 60 deg of flexion using a goniometer at the beginning of each session. All subsequently measured angles were determined by comparing the calibrated voltage output of the Biodex dynamometer to this standard position.

4.3.4 Experimental Protocol

Subjects were seated in the standard Biodex chair with the seat back positioned at 90 deg to the seat. The axis of the dynamometer was aligned as closely as possible with the axis of rotation of the knee and this alignment checked during slow passive flexion and extension movements of the dynamometer. The alignment was considered satisfactory when rotations of the dynamometer produced the minimum movement of the thigh (prior to the thigh being strapped down). Once in position, the subject was strapped down using a strap across the thigh, a waist belt and two straps diagonally across the body. The strap used to fix the shank

to the dynamometer normally has a foam pad across the shank. This padding was discarded to reduce compliance between the leg and the dynamometer.

Subjects presented for two experimental sessions, labelled Isokinetic or Isometric sessions. Each experimental session was preceded by 5 min "warm-up" consisting of passive leg extension and flexion at a rate of 60 deg s^{-1}. This "warm-up" period was used to confirm the location of knee centre.

The amplitude of NMES current was initially set at zero, then increased gradually until strong, stable, tetanic contractions of the quadriceps were produced. Current amplitude could not be equalised between subjects because of the great difference in stimulation sensitivity between subjects. For example, one subject had a stimulation threshold of 35 mA and produced strong contractions at 90 mA. Another subject had a stimulation threshold of 70 mA and required 120 mA to produce strong contractions. Current levels varied slightly between trials, presumably as a result of small changes in skin/electrode resistance and battery charge. The stimulator gave a visual indication of current level and, once a level of current was adopted for a subject, adjustments were made to the stimulator in an attempt to maintain constant current levels between trials. It was not possible to be completely constant for each trial, hence current was monitored for later analysis.

Subjects completed both isometric and isokinetic sessions as detailed below. Each condition was tested by a series of three contractions with approximately 5 min between conditions. Both active (stimulated) and passive trials were collected for each condition. This enabled the torque due to weight and passive joint resistance to be separated from the active muscle torque. Isometric contractions at 60 deg of knee flexion were repeated at intervals during each test in order to monitor the effect of fatigue throughout each session. Trials at all other angles and different speeds were randomised for each subject.

Isometric Trials:

Three contractions were performed at each knee angle with a duty cycle of 2 s stimulation followed by 2 s recovery. These were conducted at knee angles of 15, 30, 45, 60, 75 and 90

deg with repeated 60 deg contractions to assess the effect of fatigue. An example of one randomised order of data collection is illustrated by Table 4.3.4.1.

Table 4.3.4.1 Example order of collection for isometric knee angles.

Trial	Joint Angle (deg)
1	60
2	90
3	15
4	45
5	60
6	30
7	75
8	60

After the completion of testing at the above knee angles, subjects performed a fatigue protocol consisting of repeated isometric contractions at a knee angle of 60 deg for a period of 5 min. During this period, stimulation continued with the duty cycle of 2 s stimulation followed by 2 s rest. Fifteen second samples were recorded at the beginning and at 1 min intervals throughout this 5 min period.

Isokinetic Trials:

Three contractions were performed at velocities 10, 30, 60, 90, 120 and 250 deg s^{-1} with repeated isometric contractions to assess the effect of fatigue. An example of one randomised order of data collection is illustrated by Table 4.3.4.2.

Table 4.3.4.2 Example order of collection for isokinetic extension velocities.

Trial	Angular Velocity (deg s^{-1})
1	Isometric
2	120
3	90
4	Isometric
5	10
6	250
7	Isometric
8	30
9	60
10	Isometric

4.3.5 Data Collection

Signals were collected for a period of 15 s at a frequency of 1000 Hz to enable timing parameters to be measured to the nearest millisecond. During isokinetic contractions at 10 and 30 deg s^{-1}, the sampling frequency was reduced to 200 Hz to enable the longer data collection periods required to record three contractions.

During isometric trials, stimulation was delivered automatically for 2 s, with 2 s recovery between contractions. During isokinetic contractions, stimulation was controlled manually by the experimenter to produce concentric contractions during the knee extension phase. Each contraction was later checked to ensure that stimulation was initiated early enough to produce full tetanus at the 60 deg reference angle chosen for analysis.

4.3.6 Data Reduction from Isometric Trials

Variables Measured

Figure 4.3.6.1 illustrates a typical pattern from the stimulation monitoring signal. Note that the sample and hold circuit held each measured voltage until released by the following TTL pulse. For this reason, stimulation ceased at beginning of the final plateau indicated in Figure 4.3.6.1, rather than at the end. Output from the stimulation monitoring device was confirmed by running both the stimulation current and the monitoring signal through a storage oscilloscope to ensure that the recorded stimulation onset and offset times were within 1 ms of actual times.

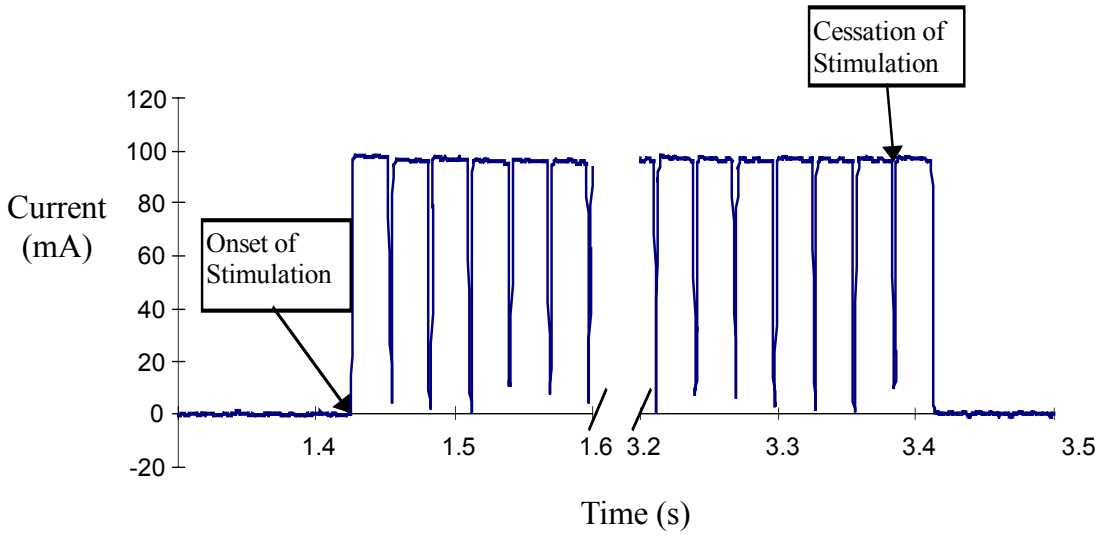

Figure 4.3.6.1 Determination of stimulation timing from stimulator output.

The ADS data collection software saved data in a coded ASCI format with four columns for dynamometer torque, stimulator current, stimulator voltage and dynamometer angle. ADS output files were unencoded using in-house software (Ana2asc, R West, The University of Sydney, 1995) and transferred to Microsoft Excel for calibration and subsequent analysis. Table 4.3.6.1 lists the parameters measured directly from the data spreadsheets.

Table 4.3.6.1 Parameters measured directly from data collected.

Knee Angle	Knee Angle was averaged over the trial.
Weight Torque	Average torque due to weight of the leg and the Biodex arm during passive trials
Time stimulation commenced (Time Stim On)	First row where stimulation current was greater than 5 mA
Average resting nett torque (Torque Rest)	Average nett torque for 1 second prior to onset of stimulation.[1]
Time torque rose above resting levels (Time Torque On)	Time when nett torque rose 0.1 N m above resting torque and remained above this level until the cessation of stimulation.[2]
Active Torque	Average nett torque between 0.5 and 1.5 seconds after the onset of stimulation. The 0.5 second delay after stimulation allowed time for torque to reach a plateau.
Time torque reached 95% of Active Torque (Time Torque Up 95%)	First row where nett torque reached 95% of the difference between Torque Rest and Active Torque.
Time torque reached 50% of Active Torque (Time Torque Up 50%)	First row where nett torque reached 50% of the difference between Torque Rest and Active Torque.
Time stimulation ceased (Time Stim Off)	The row where the last rise in current was found in the signal (Figure 4.3.6.1).
Torque at Cessation of Stimulation (Torque Stim Off)	The torque recorded at the time where stimulation ceased. This was averaged across five time periods before and after Time Stim Off in order to minimise the effect of signal noise.
Time torque declined below Torque Stim Off (Time Torque Declined)	Time where torque declined 0.1 N m below Torque Stim Off and remained below this level until the next subsequent contraction. This definition was chosen to be consistent with Time Torque On.

Time torque declined to 50% of Active Torque (Time Torque Down 50%)	First row where torque declined to 50% of the difference between Torque Stim Off and Torque Rest.
Time torque declined to 95% of Active Torque (Time Torque Down 95%)	First row where torque declined to 95% of the difference between Torque Stim Off. and Torque Rest.
Stimulation Current	Average current during active phases

Notes

1. Occasionally the sample period was less than 1 second when the first contraction commenced near to the beginning of the trial. At least 300 samples were always used for this measurement.

2. The reasoning behind this definition was as follows. Signal noise of up to 0.2 N m meant that detection of the instantaneous rise above zero was not possible. Alternative definitions for torque greater than zero could have been when torque first reached a certain percentage of maximum torque, or when it was a certain number of standard deviations above zero. The first alternative has been commonly used in previous research (eg Sahlin and Seger, 1995), however it was discarded owing to the desire to measure delay at different knee angles. The muscle length - tension relation meant that different levels of maximum torque were achieved at each length. If the torque on criteria was based on a percentage of maximum, this meant that the measured delay was seen to vary between muscle lengths simply because there was a change in the amount of torque required to be considered greater than zero.

   A similar feature was noted between subjects when a statistical measure of the zero level was used to define torque above zero (eg 3 standard deviations). There was always a small earth feedback loop in the torque signals because the Biodex dynamometer had its own specific power supply from the building. This prevented the sampling computer from being connected to the same power point. On a few testing days a higher level of noise was detected in the torque and angle signals. This was presumably due to some other equipment in the building sending a 50 Hz signal through the building's power supply, although no source could ever be found. If the statistical method was used to determine the onset of torque, the amount of torque required to be considered "on" differed between days for reasons not reflecting muscle performance.

   Another criteria tested was to take the first time torque rose above 1 N m. The 1 N m criteria provided a stable result that, although arbitrary, did not produce any artefacts in the data for reasons other than differences in the true delay between stimulation onset and torque development. This criteria was eventually discarded however, as it was clear that some of the toe region of the torque rise was being included as resting values. This meant that the rise delay was being constantly over-estimated. The method finally accepted used the last time that torque rose above 0.1 N m without falling below this level until after stimulation ceased. This criterion gave an objective measure that matched well with visual inspection of the data.

A number of variables were then calculated from the measured parameters of Table 4.3.6.1. These are listed in Table 4.3.6.2.

Table 4.3.6.2 Variables calculated from the measured parameters.

Nett Torque	Nett Torque = Active Torque - Weight Torque
Rise Delay	Rise Delay = Time Torque On - Time Stim On
Rise Time 95% (RT_{95})	Rise Time = Time Torque Up 95% - Time Torque On
Rise Rate 95% (RR_{95})	$\text{Rise Rate } 95\% = \frac{0.95\,(\text{Active Torque - Torque Rest}) - 0.1}{\text{Rise Time } 95\%}$
Rise Time 50% (RT_{50})	Rise Time 50% = Time Torque Up 50% - Time Torque On
Rise Rate 50% (RR_{50})	$\text{Rise Rate } 50\% = \frac{0.5\,(\text{Active Torque - Torque Rest}) - 0.1}{\text{Rise Time } 50\%}$
Fall Delay	Fall Delay = Time Torque Declines - Time Stim Off
Fall Time 95% (FT_{95})	Fall Time = Time Torque Off - Time Torque Declines
Fall Rate 95% (FR_{95})	$\text{Fall Rate}95\% = \frac{0.95\,(\text{Torque Stim Off - Torque Rest}) - 0.1}{\text{Fall Time } 95\%}$
Fall Time 50% (FT_{50})	Fall Time 50% = Time Torque Down 50%- Time Torque Declines
Fall Rate 50% (FR_{50})	$\text{Fall Rate}50\% = \frac{0.5\,(\text{Torque Stim Off - Torque Rest}) - 0.1}{\text{Fall Time } 50\%}$
Max Torque	Maximum Nett Torque recorded by a subject at any knee angle.

The stimulator was designed to produce a constant voltage output, and therefore variations in current were possible where impedance between the stimulation electrodes changed during

the experiment. Trials with currents later found to deviate more than 7% from reference values were discarded from the analysis. The average absolute deviation of all trials from the reference values was 1.4%.

4.3.7 Data Reduction from Dynamic Trials

Data were analysed for dynamic trials from three complete flexion and extension movements of both active and passive movements. The following variables were determined from these trials.

Weight Torque

Weight torque was determined by fitting data from the passive 10 deg s^{-1} trial to Equation 4.3.7.1.

$$y = a + b\,Cos(\theta)$$

Equation 4.3.7.1

y is torque, θ is knee angle, a and b are constants

The 10 deg s^{-1} velocity was chosen because the effects of viscous resistance would be least. Note that there was still some passive joint torque present as indicated by the hysteresis loop during knee flexion and extension (Figure 4.3.7.1). The weight torque equation was determined by fitting the equation to both flexion and extension curves. This procedure assumed that there was equal passive resistance to both flexion and extension, however the difference between flexion and extension curves was quite small (Figure 4.3.7.1). Only mid range joint angles were used to determine the weight curve for two reasons. Firstly, there was more likely to be passive resistance at the end of range. Secondly and more importantly, the Biodex machine had to slow before it reached the end of range before it stopped. Inertial forces during the deceleration produced obvious deviations from the weight torque's cosine curve and hence had to be eliminated from the fitted data.

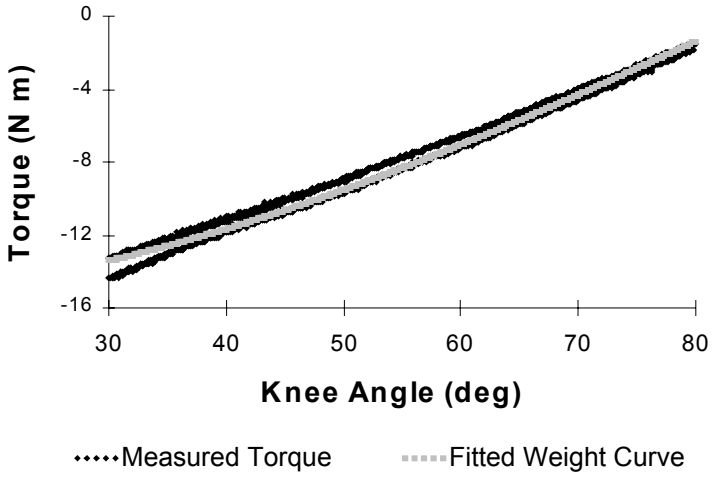

Figure 4.3.7.1 Weight torque fitted to passive data collected at 10 deg s^{-1} for one exemplar subject.

Passive Torque

Passive joint torque was calculated as the weight torque (as a function of knee angle) subtracted from the actual torque measured during each passive trial.

Weight Torque and Passive joint torque at the reference angle of 60 deg were calculated by averaging across all data points where the knee was extending and the knee angle was between 59.5 and 60.5 deg.

Active Torque

Active torque was recorded when the knee angle was between 59.5 and 60.5 deg. Trials were included only when stimulation was on during these angles and when stimulation had been on for at least 100 ms before this angle to allow time for muscle force to build up. Torque was recorded separately for the three contractions present within each trial.

Nett Torque

Nett Torque = Active Torque - Passive Torque

4.3.8 Statistical Analyses

The effect of knee angle on isometric muscle performance parameters from Table 4.3.6.2 were analysed by Linear Regression using Knee Angle, Knee Angle Squared and Max Torque as predictors. Linear Regression was performed using a forwards stepping strategy whereby predictors were entered sequentially in descending order of their correlation to the dependent variable.

Stimulation changes with fatigue were assessed by including the first 60 deg test at the beginning of each session, together with six time periods during the fatigue protocol (0, 1, 2, 3, 4 and 5 min). This gave seven levels for repeated measures ANOVAs with time as the independent variable. Repeated within-subjects contrasts were conducted between each of the seven time scores.

Changes in active and passive torques with joint angular velocity were assessed from the dynamic trials using repeated measures ANOVAs with velocity as the independent variable. Seven levels of velocity were included for the active torque including isometric contractions at 0 deg s^{-1}. Only six levels were used for the passive torques because, by definition, passive torque had to be equal to weight torque during isometric contractions. Simple within-subjects contrasts were performed to compare each scores at each velocity with either the isometric condition for active torques or 10 deg s^{-1} for passive torques.

SPSS (9.0 or 10.0) was used for all statistical comparisons and the 0.05 level adopted for statistical significance. For those cases violating the assumption of equal variance between cells, significance was established using a Greenhouse-Geisser adjustment (Vincent, 1995).

4.4 Cycling Experiments

4.4.1 Equipment

The MOTOmed viva (Reck Medizintechnik, Betzenweiler, Germany) is a cycle ergometer designed specifically for rehabilitation of mobility impaired patients (Figure 4.4.1.1). The

ergometer utilised a motor to provide passive leg movement for those patients without the capacity to cycle unaided. For subjects strong enough to pedal against some force, the motor provided resistance by acting as a DC generator and generating rather than drawing electrical current. Computer monitoring of the crank velocity aimed to achieve constant cycling velocity by regulation of the motor's current.

Figure 4.4.1.1 The MOTOmed Viva cycle ergometer.

Foot plates were used in place of regular pedals on the MOTOmed ergometer. This ensured that the feet were held safely in place without the need for subject coordination. Constant monitoring by the ergometers on-board computer halted the motor if a sudden increase in resistance occurred as a result of muscle spasms. The computer control also enabled users to select a desired velocity of rotation and maximum cycling resistance. The ergometer conformed to standards for medical electrical devices set by the European Community's Medical Devices Directive.

As can be seen in Figure 4.4.1.1, the MOTOmed ergometer could be used with any chair. There were a number of requirements when choosing a suitable chair for this experiment. The chair had to be:

a) Softly padded to reduce the possibility of pressure sores.
b) Low enough so that the thighs were off the seat at the most extended position (thighs contacting the chair would have induced torque about the hip joint that would then need to be accounted for in the model.
c) Vinyl covered because some subjects did not have complete bladder control, especially under the influence of NMES.
d) Clamped into position so that the relative position of the chair and cycle crank remained constant (the MOTOmed is light enough to slide forward unless clamped)

Figure 4.4.1.2 shows a subject in the chosen chair.

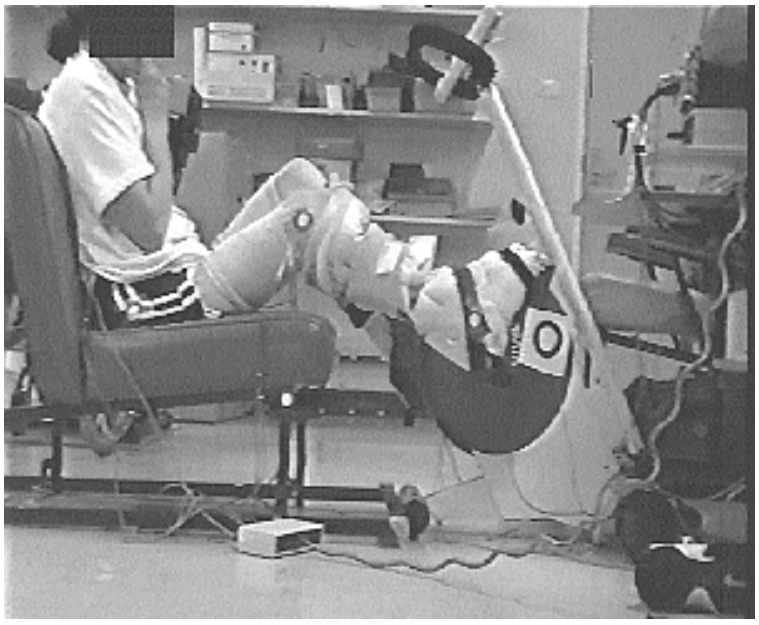

Figure 4.4.1.2 Cycling using the MOTOmed Viva and chosen chair.

SCI subjects had to be braced in some way to prevent lateral movement of the legs during cycling; the MOTOmed had braces arising from the foot plates that were strapped to the calves (Figure 4.4.1.3). The calf braces also fulfilled the purpose of preventing movement of

the ankle joint. This ensured that the legs conformed to the two segment leg model described in section 3.2.

Foam padding was used between the calf brace and the leg so that the legs could be held firmly in place with elastic bandages without causing skin irritations in subjects with poor blood supply. Subjects wore soft foam booties (Figure 4.4.1.3) within a harder foam shell produced for the Ergys ergometer. The foam shells enabled the feet to be strapped tightly into the MOTOmed foot plates without compromising circulation of the feet.

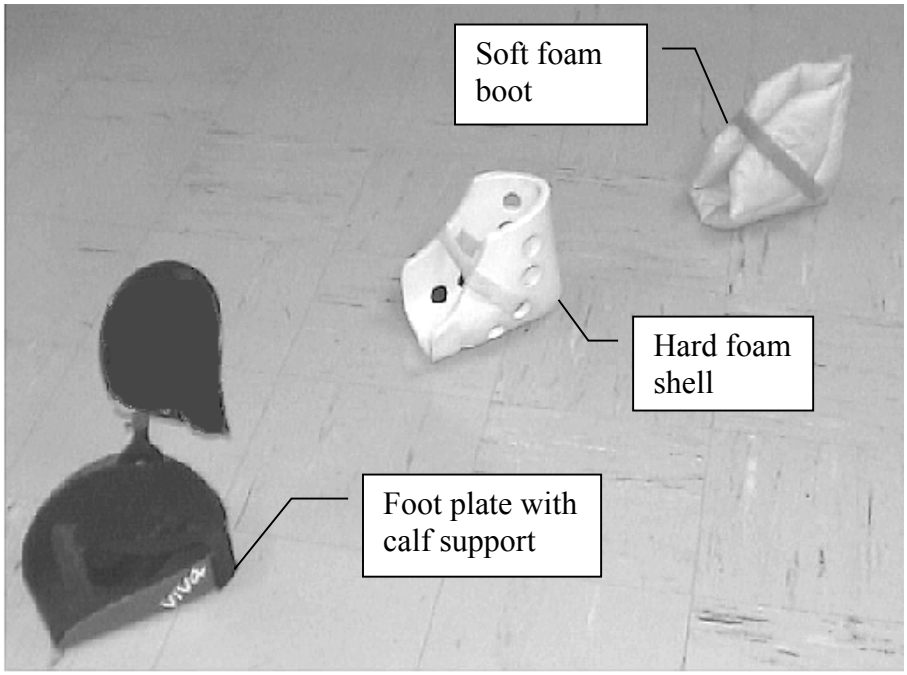

Figure 4.4.1.3 Leg bracing system used with the cycle ergometer.

The MOTOmed ergometer provided output of crank angle, and motor current via an RS232 interface to a IBM compatible personal computer (Celeron 333 MHz) running Labview Software (Version 4.01, National Instruments Corp). Labview software (C Fornusek, The University of Sydney) sampled crank angle and used this to control the laboratory muscle stimulator described in Section 4.3.1. Stimulation could be set to commence and cease at specific crank angles from the Labview front panel. A signal corresponding to motor current was also sent by the MOTOmed ergometer and displayed on the front panel. This enabled some indication of the torque produced by the cyclist during the data collection period.

The MOTOmed ergometer delivered digital information to the Labview program at intervals approximately 16 ms apart, however the rate of delivery was not constant. The maximum time delay between information updates was generally less than 26 ms. To reduce the effect of sampling delay on error in switching on the stimulator, the software used angular velocity to predict occurrence of angles when stimulation should commence and cease.

As with the isokinetic knee extension experiments, constant voltage, monophasic, square wave stimulation pulses of 250 μs were delivered at a frequency of 35 Hz. Self adhesive electrodes (8 × 13 cm, Empi, Cat No 86906350 for quadriceps and hamstrings; 5 × 9 cm, Empi, Cat No 86905240 for gluteals) were moistened then placed over the mid-bellies of the quadriceps, hamstrings and gluteal muscles (Figure 4.4.1.4). Current was slowly increased while the subject was cycling until strong contractions were visible on the Labview torque display. Maximum current was limited to 140 mA.

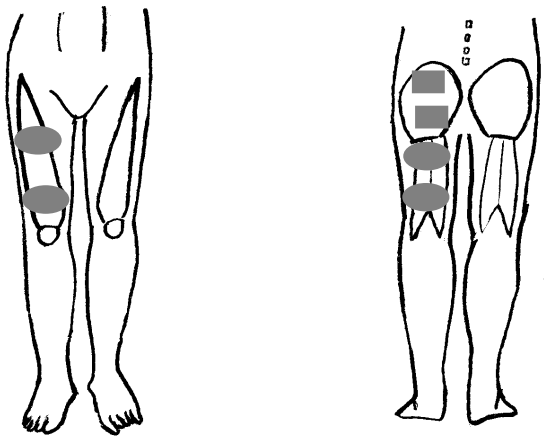

Figure 4.4.1.4 Illustration of electrode placements.

The MOTOmed foot plates were attached to force transducer pedals designed by Newmiller et al. (1988). These pedals had previously been used by Sinclair et al. (1996) to record forces for SCI individuals cycling an Ergys ergometer. The pedals generated voltages proportional to applied shear and normal forces that, on each day of testing, were calibrated by applying

known weights within the range of forces recorded during cycling. The output of the pedal transducers was linear with an R^2 value of better than 0.99 for both shear and normal forces (see Appendix 3.2 for example calibration).

The angle between the pedal and crank was measured using rotary potentiometers attached to the axle of the force transducer pedals (Newmiller et al., 1988). Appendix 3.2 also gives an example calibration for pedal angle which was achieved by placing the pedals in known positions using a spirit level. The potentiometers were linear with R^2 always greater than 0.999.

Voltages from the force and angle channels of the pedal transducers were low pass filtered at 25 Hz and then sampled at a frequency of 250 Hz using an IBM compatible personal computer (Intel 80386), 12 bit analogue to digital converter (DT2801, Data Translation) and ADS software (Motion Analysis Corp). The high sample frequency was chosen because of a 50 Hz signal passing through the low pass filters. Sampling at 250 Hz allowed the 50 Hz noise to be removed by post-collection processing. The filters, although allowing this 50 cycle noise to pass through, were essential because of high frequency noise (> 1000 Hz) that was otherwise recorded from the pedal transducers.

The available analogue to digital converter was not compatible with the Labview software used to sample digital signals from the MOTOmed and control stimulation timing. Separate computers were therefore used to collect the analogue and digital signals. Crank angles digitally sampled from the MOTOmed were essential to calculate global pedal position from the pedal-crank angles recorded from the analogue signals. It was therefore necessary to match the data collection times of both computers. To facilitate time synchronisation, a switch on the MOTOmed generated a 5 V signal at a crank angle of 320 deg in each revolution. This switch pulse, together with the time code attached to each sample recorded by the Labview application, enabled the two signals to be time matched. This process is described fully in section 4.4.3. A further check of this process was achieved by the Labview application generating a 5 V signal whenever the stimulation was switched on. This enabled the time coding to be checked as well as providing an accurate recording of when stimulation commenced and ceased during each trial.

In summary, two computers were used to collect data during the cycling experiments. Computer 1, using a Labview application, recorded digital signals from the MOTOmed giving crank angle and an estimate of torque generated from the current drawn by the ergometer's motor①. This data was collected at irregular intervals at an average frequency of 64 Hz together with a time code for each sample collected. Computer 1 also controlled the stimulator output② and generated a DC voltage③ whenever the stimulation was switched on. Computer 2 collected analogue signals from the pedals' force and angle transducers④ , together with signals indicating the onset of stimulation from Computer 1③ and a switch corresponding to a known crank angle from the ergometer⑤ (The numbers in this paragraph refer to components illustrated in Figure 4.4.1.5).

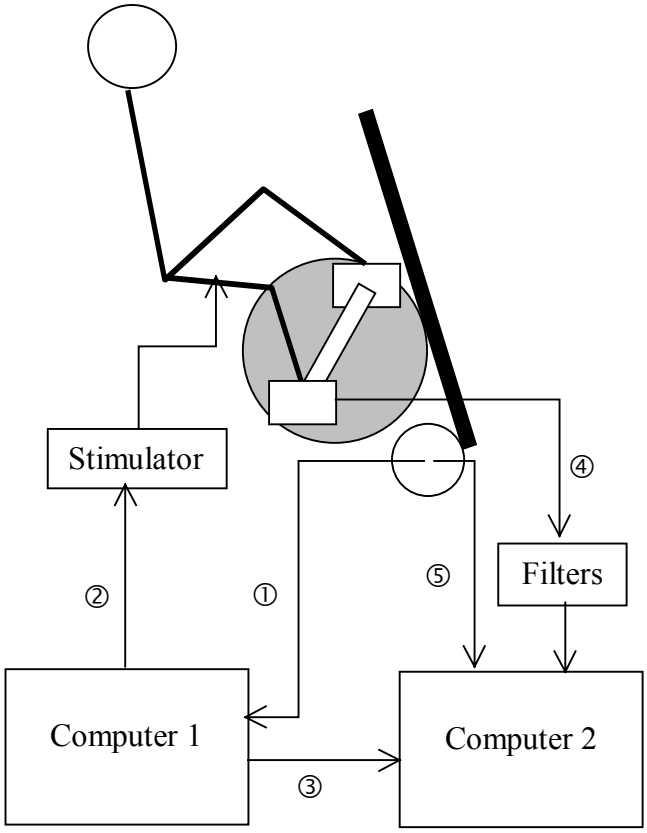

Figure 4.4.1.5 Illustration of the major data collection components. See text for description of components ① to ⑤.

Circular markers were placed over the greater trochanter and knee of each subject. Additional markers were placed on the pedal axle and on the foot shell in a location approximating the location of the lateral malleolus (Figure 4.4.1.2). Subjects were filmed while cycling using a PAL video camera operating at 50 fields per second. The markers were subsequently digitised using an APAS digitising system (Ariel Dynamics, Trabuco Canyon, California). There was no direct synchronisation between the film and force measurements, however Computer 2 beeped following collection allowing approximate identification of data collection times. The digitised co-ordinates were collected primarily to determine hip and crank locations as inputs to the kinematic model. Complete data synchronisation was therefore not required. The approximate synchronisation did at least allow film to be collected during both active and passive cycling for comparison between the two.

4.4.2 Subjects

Seven subjects with SCI (2 female, 5 males) were recruited for the cycling experiments. Five of these had previously completed the knee extension experiments two years previously. All subjects had lesions between T4 and T8 and were classified as ASIA-A (6) or ASIA-B (1) (Ditunno et al. 1994). Subjects again underwent informed consent procedures according to the guidelines of The University of Sydney Human Ethics Committee.

4.4.3 Experimental Protocol

Subjects presented for three experimental sessions. Before each session, subjects lay on a plinth while electrodes were placed over the muscles. Subjects then transferred into the ergometer chair where the seat position was adjusted at the first session. The chair was moved so that the subjects' knees were approximately 45 deg at their most extended position. The ergometer motor was used for five min of passive cycling after which stimulation current was adjusted until strong contractions were recorded by Computer 1.

The first session consisted of 5 min continuous cycling with stimulation of only the right quadriceps muscles at firing angles of 300 to 20 deg from TDC. Data were collected for 20 s periods at the beginning of the cycling period and at 1 min intervals thereafter.

The second session involved a searching strategy to identify the stimulation onset and cessation angles that maximised acute power output of each muscle group. The ergometer motor maintained cycling at 50 rpm throughout the session, while stimulation was applied to single muscles for periods of 10 s and data collected during the stimulation periods. At approximately 45 s intervals, the stimulation firing angles were changed and 10 s stimulation periods repeated throughout the session. A searching strategy will be described below to explain how firing angles were chosen during this session. The searching strategy was applied sequentially to the quadriceps, hamstrings and gluteal muscles during this session. In total, approximately 80 - 100 trials were collected for each subject during session two. As each trial generated information on two computers, sampling respectively five channels at 64 Hz and eight channels at 250 Hz; the amount of data generated was substantial.

Session three was a repeat of the second session with the chair was moved backward 3 - 5 cm. It was initially planned to move the chair back 5 cm for all subjects, however two subjects with shorter legs were no longer able to reach the pedals with a 5 cm shift. The decision was taken to move the seat backwards rather than forwards because the amount of hip and knee flexion already exceeded the range for moment arm data available in the literature. Moving the seat forward would have required an even greater extrapolation of moment arms outside the range of knee angles for which moment arm data was available.

Searching Strategy

The second and third cycling sessions were designed to identify stimulation firing angles that maximised work done on the ergometer cranks. Section 4.4.4 explains how this was examined during subsequent analysis of the data, however complex analyses could not be performed during data collection. During each session, it was necessary to estimate the peak firing angles so that angles either side of peak were available for subsequent processing. A searching strategy was therefore employed to estimate peak firing angles during the second and third sessions.

The aim was to find stimulation firing angles that applied an initial negative torque on the crank, as illustrated by Figure 4.4.3.1b. Production of negative torque after stimulation onset would indicate that stimulation was commencing too soon and retarding propulsion. After each stimulation period, the resulting crank torque pattern from Computer 1 was inspected for

the production of negative torque during the initial period of torque generation. If no initial negative torque was observed, the stimulation onset angle was advanced for the subsequent stimulation period. This process was treated cautiously to avoid large periods of eccentric force being applied by a muscle. It was anticipated that each subject would exhibit quite different angles where torque changed from positive to negative, so there were no prescribed angles set in advance for all subjects. Rather, firing angles were advanced cautiously during each session looking for a negative torque pattern like that in Figure 4.4.3.1b. The Labview front panel assisted this process by estimating average power output for each revolution. Advancing the firing angle would be expected to increase power output if there was no negative torque developed. Once firing angles started to produce negative torque then the power output would be expected to fall with further stimulation advancement.

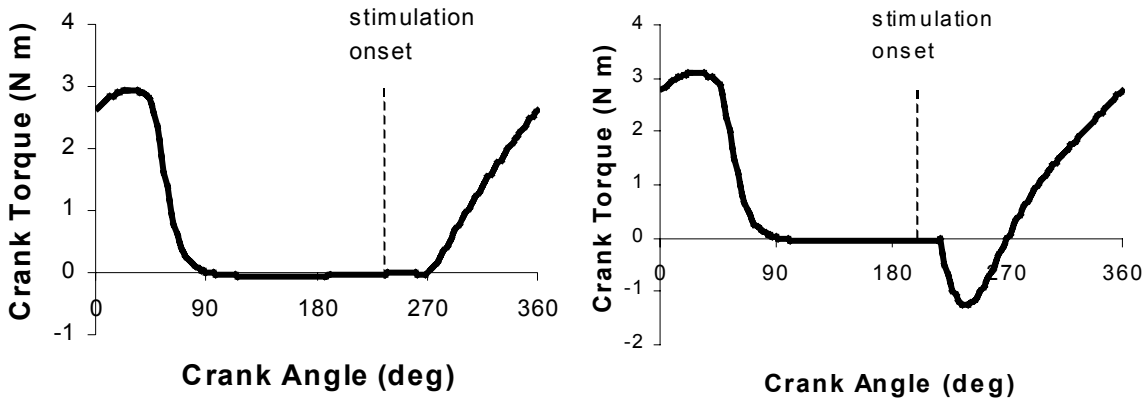

a) Stimulation commences after the period that would have developed negative torque.

b) Stimulation commences earlier, during the period that develops negative torque.

Figure 4.4.3.1 Illustration of negative torque pattern with early stimulation onset..

The process of identifying the peak stimulation firing angles was made difficult by two inherent problems. Firstly, progressive fatigue often resulted in a reduction in power, even when no negative torque was recorded. Secondly, the torque patterns displayed by Computer 1 were only estimates derived from the current generated by the ergometer motor, and subtracted from currents generated during passive cycling. If a subject moved after the recording of passive torque levels, this resulted in curves that did not display zero torque,

even when the muscles were inactive. This meant that there was some guesswork associated with deciding when the stimulation had been advanced too far. To help resolve this issue during post-processing, the data collection period was increased to 12 s whilst maintaining a stimulation duration of 10 s. This enabled a passive period to be collected within every sample, and so improved the match between active and passive trials when the muscle was switched off. This process was commenced only after the second subject had been tested and found to exhibit large changes from passive levels, making the calculation of nett torques inaccurate. For all subsequent subjects, post-processing allowed a more accurate match between the active and passive components within each trial. This did not, however, improve the data viewed from Computer 1 during the actual collection period because the data could not be processed in real time. It will be seen in Chapter 7 that the searching strategy was successful in identifying peak stimulation angles for the majority, but not all cases.

Once an initial period of negative torque was identified for a muscle, the firing angle was progressively retarded to pass back over that angle as an additional check that peak power was achieved. The process was then repeated to find the maximum angle where stimulation could be turned off. See section 7.2.2 for further discussion of features making identification of the peak angle difficult.

4.4.4 Data Analysis

As described earlier, the Labview program operating on Computer 1 collected digital signals from the MOTOmed ergometer at irregular intervals consisting of the ergometer velocity, motor current and crank angle; together with the time each data point was received. The ASCII file containing these data was imported to a spreadsheet for further analysis (Microsoft Excel). Calibration equations were applied to the angle and velocity signals and the angle signal converted to a cumulative angle, rather than resetting to zero deg after each TDC. Cubic splines were then fitted to the calibrated signals as functions of collection time using an Excel Add-In function (Spline97,C Co, The University of Delaware, 1997). These spline functions were used to interpolate the angle and velocity signals at a regular frequency of 250 Hz, to match the sampling frequency of Computer 2.

ASCII files from Computer 2 contained shear and normal forces as well as pedal angles with respect to the cranks. The output files from Computer 2 also contained data generated by

Computer 1 indicating when the stimulation was switched on and off; a signal from the ergometer that switched from zero to 5 V at a crank angle of 320 deg; and a time code with an arbitrary first time and each subsequent sample being spaced 1/250 s apart. Force and pedal angle signals were respectively transformed to values in Newtons and degrees by applying the previously described calibration equations.

Crank angles from the Computer 1 output file were imported to the Computer 2 file by ensuring that the time of each crank angle reaching 320 deg on Computer 1 matched the time when the ergometer switch changed from 5 to 0 V on Computer 2. The time of Computer 2's first sample was adjusted to minimise the sum of squares difference between the times where each computer registered the angle as passing 320 deg.

The process of combining data from each computer's output was necessary to give a measure of crank angle corresponding to each data point in the Computer 2 files. The absolute angle of the pedal was calculated by adding the pedal angle with respect to the crank to the crank angle at that time. The pedal angle with respect to the crank was measured using a rotary potentiometer attached to the pedal axle. Within each revolution of the potentiometer, the signal was lost for approximately 10 deg while the potentiometer returned from maximum resistance back to minimum resistance. Pedal angles during this small period were calculated by linear extrapolation from previous angles (Newmiller et al., 1988) before calculation of the absolute pedal angle.

Finally, all force data were passed through a zero lag 4^{th} order Butterworth filter with a cut-off frequency of 10 Hz. The 10 Hz frequency was chosen after performing a residual analysis as described by Winter (1990). Appendix 3.3 gives an example output from the residual analysis.

The DC voltage generated by Computer 1, that switched on and off as stimulation to a muscle was activated, enabled post-hoc measurement of the crank angles through which stimulation was active. The angle of stimulation cessation could not be determined with a precision of better than 8.5 deg because of the nature of the stimulation as discrete pulses at a frequency of 35 Hz. During 1/35 of a second, the crank would rotate through an angle of 8.5 deg when rotating at 50 rpm. If post-hoc measurement indicated that stimulation ceased at a specific angle, the last stimulation pulse may therefore have been up to 8.5 deg before this angle.

Horizontal and vertical forces applied to the pedals were calculated from the shear force, normal force and pedal force according to Equations 4.4.4.1 and 4.4.4.2. The direction of all pedal forces[2] are illustrated by Figure 4.4.4.1. Torque applied to the crank was then calculated using equation 4.2.3.9.

$$F_x = -F_{norm} \times \mathrm{Sin}(pedang) + F_{shear} \times \mathrm{Cos}(pedang)$$

Equation 4.4.4.1

$$F_y = F_{norm} \times \mathrm{Cos}(pedang) + F_{shear} \times \mathrm{Sin}(pedang)$$

Equation 4.4.4.2

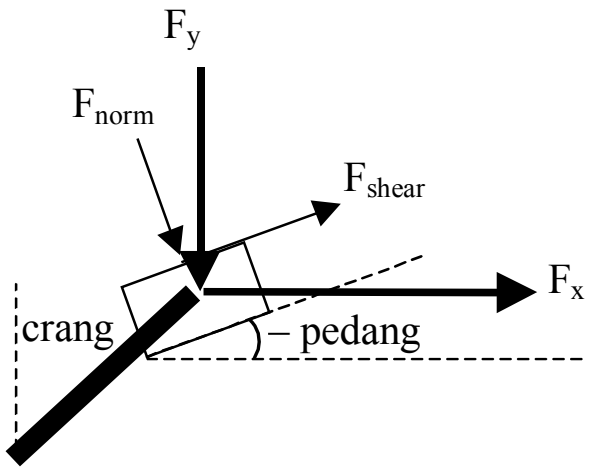

Figure 4.4.4.1 Calculation of pedal forces and angles. Note that a positive pedal angle would have been inclined forward, however the pedal was always inclined backward. Consequently, the illustration shows a negative pedal angle.

For each trial, nett pedal forces were calculated by subtracting the forces measured at each crank angle during passive cycling from the active pedal forces. The passive forces were

[2] Vertical pedal force (fpy) is given as positive downwards within this section, as illustrated by Figure 4.4.4.1. The model described in Section 4.2 and included within Appendix 2.1 used an upwards positive convention for pedal forces. Care was taken always to convert modelled pedal forces to the measured convention before comparison of the two.

measured in two ways. The first method involved collecting whole trials of passive cycling and averaging the passive forces at each crank angle throughout the trial. This method was used during the fatigue protocol for every subject and for the angle seeking protocols of the first two subjects. Passive force levels would change, however, if there was any movement of the subject's position over time. One subject in particular demonstrated larger changes in passive levels than had previously been observed. After post-collection analysis of this subject's data, it was decided to change the procedure for collecting passive levels. For each subsequent test, the duration of data collection was increased from 10 s to 12 s and the stimulation switched off during the final 2 s. For these trials, the last revolution was taken as the passive level and therefore subtracted from all data during the first 10 s.

Instantaneous power output (W) was calculated as the product of nett crank torque (N m) and angular velocity of the crank (rad s^{-1}). Average power output was calculated for each trial by averaging instantaneous powers across six complete revolutions.

A non-linear analysis of regression was performed to identify the crank angles producing peak power outputs from the angle seeking experiments. SPSS 10.0 was used to identify regression constants for a quadratic fit of stimulation angle to power output. Six separate regressions were performed for the onset and cessation of stimulation for quadriceps, hamstrings and gluteal muscles. Equation 4.4.4.3 was used to conduct a non-linear Analysis of Regression. Constants a and b were fitted using all subjects to identify the stimulation angles producing maximum stimulation. The exponential function with constant d_i was included to account for progressive fatigue with each trial throughout a day's experiment. Separate constants c_i and d_i were fitted for each subject on each day to account for differences in strength and rate of fatigue.

$$\text{Power} = a \times \text{stimon} + b \times \text{stimon}^2 + c_i + e^{d_i \times \text{trial}}$$

Equation 4.4.4.3

After the determination of constants a and b, peak angle was identified as the maximum of Equation 4.4.4.3, using Equation 4.4.4.4.

$$\text{Peak Angle} = \frac{-a}{2b}$$

Equation 4.4.4.4

Analysis of Regression gave a standard error of the estimate for constants a and b. An estimate of the potential error in calculating peak angle that results from the uncertainty in constant a may be derived by taking the partial derivative of Equation 4.4.4.4 with respect to constant a, and multiplying this by a measure of uncertainty for constant a (Kirkup, 1994). This was performed similarly for constant b, using the standard error of the estimate as the uncertainty for each constant, to produce Equations 4.4.4.5 and 4.4.4.6.

$$\text{Error}_a = \frac{-1}{2b} \times \text{SEE}_a$$

Equation 4.4.4.5

$$\text{Error}_b = \frac{a_1}{2b^2} \times \text{SEE}_b$$

Equation 4.4.4.6

The following procedure was used to compare crank torques predicted by the computer simulations with those calculated from measured pedal forces. Tables were produced giving the predicted and average measured crank torques for every even crank angle between 0 and 360 deg. Pearson's product moment correlation was calculated to indicate the similarity between measured and predicted crank torques.

In order to decide whether the model's performance changed with stimulation firing angle, six representative stimulation angles were chosen for each muscle. Because different stimulation angles were measured for each subject, representative angles were chosen that gave the largest number of subjects using those angles. A one-way repeated ANOVA with repeated measures was performed for each muscle to assess whether the model's ability to predict crank torques changed with stimulation angle. For those cases violating the assumption of equal variance between cells, significance was established using a Greenhouse-Geisser adjustment (Vincent, 1995).